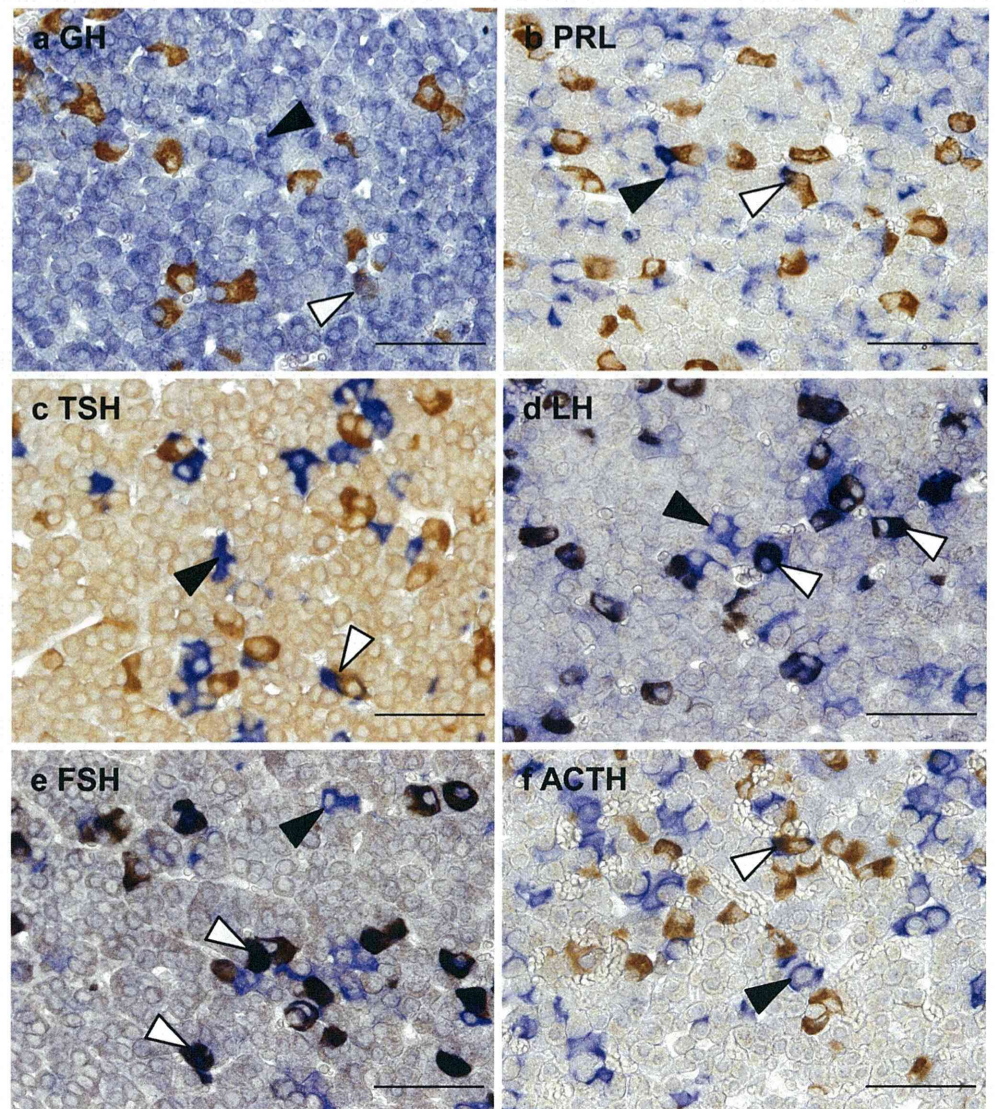


staining for SCGB3A2 and pituitary hormones was performed. SCGB3A2 was well co-localized with gonadotrophs expressing LH and FSH and double-immunopositive cells were found at 47.3 %±9.9 and 48.7 %±7.7 %, respectively (Fig. 4; Table 2). GH-, PRL-, TSH- and ACTH-immunopositivity was found in 5.1 %±1.4, 1.5 %±0.2, 5.8 %±0.6 and 14.4 %±1.3 % of SCGB3A2-immunopositive cells, respectively (Fig. 4; Table 2).

Effects of SCGB3A2 stimulation on mRNA expression of gonadotrophs

To clarify the role of SCGB3A2 expressed in the anterior pituitary gland, the effect of SCGB3A2 on mRNA expression of LH and FSH in primary cultured cells of the rat anterior pituitary was investigated using qPCR. Stimulation of SCGB3A2 (300 ng/ml) significantly inhibited LH and FSH expression ($P<0.01$) (Fig. 5).

Fig. 4 Double staining of SCGB3A2 and anterior pituitary hormones in the adult mouse pituitary gland. Immunohistochemistry for SCGB3A2 and growth hormone (a), prolactin (b), thyroid-stimulating hormone (c), luteinizing hormone (d), follicle-stimulating hormone (e) and adrenocorticotropic hormone (f). Brown signal indicates SCGB3A2, whereas blue signal indicates anterior pituitary hormones. Black arrowheads indicate immunopositive cells for anterior pituitary hormones and white arrowheads indicate double-positive cells for SCGB3A2 and anterior pituitary hormones. Bars 50 μ m



Discussion

This is the first report showing the presence of SCGB3A2 in the mouse pituitary gland. In this study, immunohistochemistry and RT-PCR revealed that SCGB3A2 is expressed in both the anterior and posterior lobes of the pituitary gland, whereas NKX2-1 is expressed only in the posterior lobe, as previously reported (Nakamura et al. 2001). Considering that SCGB3A2 is a direct target for NKX2-1 (Niimi et al. 2001; Tomita et al. 2008), these results suggest that SCGB3A2 expression is regulated by transcription factors other than NKX2-1 in the anterior lobe of the pituitary gland. Indeed, it was reported that *C/EBP α* and *C/EBP δ* regulate *Scgb3a2* transcription in mice by binding to specific sites located in the *Scgb3a2* promoter and the activity is synergistically enhanced through cooperative interaction with NKX2-1 (Tomita et al. 2008). *C/EBPs* are a family of transcription factors containing the basic leucine zipper (bZIP) domain at the C-terminus that is involved in

Table 2 Immunohistochemical co-localization of SCGB3A2 and pituitary hormones

	Hormone					
	GH	PRL	TSH	LH	FSH	ACTH
SCGB3A2-expressing cells (%)	5.1±1.4	1.5±0.2	5.8±0.6	47.3±9.9	48.7±7.7	14.4±1.3

The adult mouse pituitary glands were immunostained with SCGB3A2 and each anterior pituitary hormones-specific antibody and immunopositive cells of 5 fields of $\times 400$ magnification were counted. Nearly half of the SCGB3A2 immunostained cells were LH- and FSH-positive and to some extent ACTH-positive

Few SCGB3A2 immunostained cells were positive for GH, PRL and TSH. GH, LH, FSH, ACTH, $n=4$; TSH, $n=5$; PRL, $n=8$

dimerization and DNA binding (Ramji and Foka 2002). Six members of the family, C/EBP α , β , γ , δ , ϵ and ζ , have been identified to date and they play pivotal roles in controlling cellular proliferation and differentiation, metabolism, inflammation and numerous other responses, particularly in hepatocytes, adipocytes and hematopoietic cells (Ramji and Foka 2002). Few studies have investigated the potential roles of C/EBPs in pituitary cell lines. For example, C/EBP α was

detected in extracts of GH-secreting GC cells and prolactin-secreting 235-1 cells (Lew et al. 1993). In addition, expression of exogenous C/EBP α in GHFT1-5 cells activated a co-transfected GH gene promoter (Schaufele et al. 2001) and prolonged the cell cycle (Liu et al. 2002). Furthermore, C/EBP α and Pit-1 cooperated in the activation of both PRL and GH transcription (Schaufele et al. 2001; Enwright et al. 2003). Finally, C/EBP β and C/EBP δ were shown to activate the clusterin promoter and induced clusterin protein expression was evident in gonadotroph cells and pituitary tissue overexpressing pituitary tumor transforming gene (PTTG) (Chesnokova et al. 2011). These reports indicate that C/EBPs are important for control of expression of pituitary hormones; however, to the best of our knowledge, C/EBP expression in the mouse pituitary gland has not been previously reported. In this study, C/EBP β , γ , δ and ζ were clearly expressed in the adult mouse pituitary gland. Taken together, these studies suggest that C/EBPs and/or C/EBP-regulated pituitary-specific transcription factors may regulate *Scgb3a2* transcription in the pituitary gland, particularly in the anterior lobe of the pituitary gland.

SCGB3A2 expressed in the anterior pituitary gland co-localized with gonadotrophs in adult and neonatal mice and SCGB3A2 suppressed the expression of LH and FSH mRNAs in primary cultures of rat pituitary cells. These results suggest that SCGB3A2 may regulate FSH/LH production in an autocrine or paracrine manner. SCGB3A2 is a secreted protein and exhibits growth factor, anti-inflammatory and anti-fibrotic activities (Chiba et al. 2006; Kurotani et al. 2008; Kurotani et al. 2011). However, the mechanisms of these activities, including the involvement of a possible SCGB3A2 receptor, have not been elucidated. Macrophage scavenger receptor with collagenous structure (MARCO) expressed in alveolar macrophages in the lungs has been suggested to be a receptor for SCGB3A2 (Bin et al. 2003); however, one report identified a possible SCGB3A2-specific receptor on the mesenchymal cells of mouse fetal lungs where MARCO could not be found (Kurotani et al. 2008). Therefore, further studies are required to understand the mechanisms of action of SCGB3A2 including identification of its receptor(s) and the downstream associated signaling pathways.

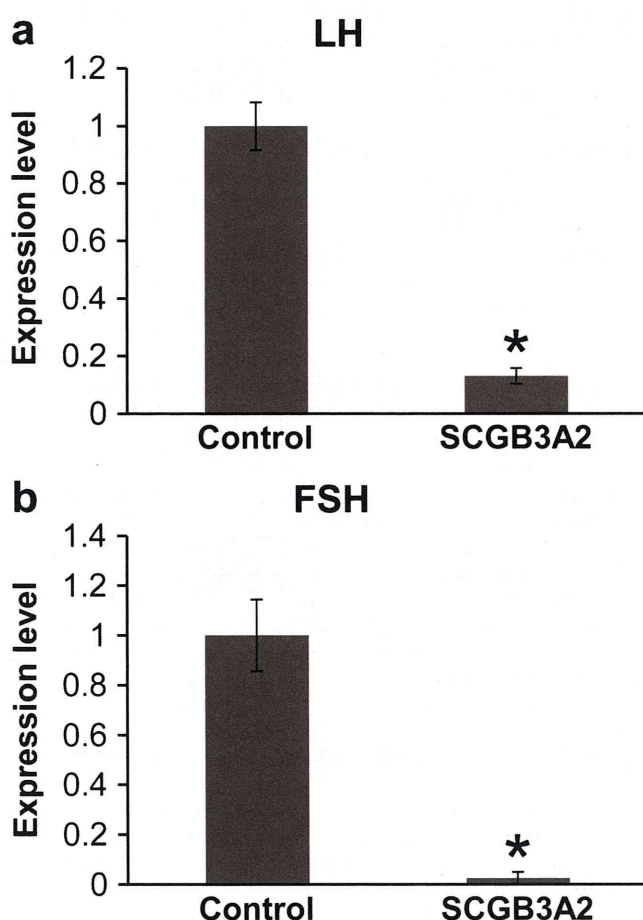


Fig. 5 Effects of SCGB3A2 stimulation on mRNA expression of anterior pituitary hormones in primary cultured rat pituitary cells. Rat anterior pituitary cells were cultured and stimulated by SCGB3A2 (300 ng/ml) for 24 h and mRNA were extracted. Expression of LH (**a**) and FSH (**b**) was quantified by real-time RT-PCR. Expression levels of LH and FSH were significantly inhibited by SCGB3A2 stimulation. * $P<0.01$; $n=6-8$

The finding that both NKX2-1 and SCGB3A2 are expressed in the posterior lobe of the pituitary suggests that NKX2-1 regulates *Scgb3a2* transcription in the posterior pituitary and thus may have a role in posterior pituitary function. In rats, NKX2-1 is expressed in the pituicyte of the posterior lobe (Nakamura et al. 2001). Although pituicytes are the astrocyte-type glial cells that have long been suspected of having a role in regulating the secretion of neurohypophysial hormones (Leveque and Small 1959), the exact function of the pituicyte and the role of NKX2-1 in the pituicyte remain unknown. It would be interesting to investigate the role of NKX2-1 and/or SCGB3A2 in the regulation of neurohypophysial hormone release.

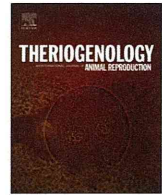
In conclusion, SCGB3A2 may regulate FSH/LH production in the anterior lobe of the pituitary gland and transcription factors other than NKX2-1 likely control expression of *Scgb3a2* in this organ.

Acknowledgments We thank Ms. Sayaka Komino (Yamagata University) and Dr. Ken Fujiwara (Jichi Medical University) for technical support and advice. This study was supported by a Grant-in-Aid for Young Scientists (C) and by the Dissemination of Tenure Tracking System Program of Ministry of Education, Culture, Sports, Science and Technology-Japan.

Open Access This article is distributed under the terms of the Creative Commons Attribution License, which permits any use, distribution and reproduction in any medium, provided the original author(s) and the source are credited.

References

- Bin LH, Nielson LD et al (2003) Identification of uteroglobin-related protein 1 and macrophage scavenger receptor with collagenous structure as a lung-specific ligand-receptor pair. *J Immunol* 171(2): 924–930
- Chesnokova V, Zonis S et al (2011) Lineage-specific restraint of pituitary gonadotroph cell adenoma growth. *PLoS ONE* 6(3):e17924
- Chiba Y, Kurotani R et al (2006) Uteroglobin-related protein 1 expression suppresses allergic airway inflammation in mice. *Am J Respir Crit Care Med* 173(9):958–964
- Enwright JF 3rd, Kawecki-Crook MA et al (2003) A PIT-1 homeodomain mutant blocks the intranuclear recruitment of the CCAAT/enhancer binding protein alpha required for prolactin gene transcription. *Mol Endocrinol* 17(2):209–222
- Fujiwara K, Kikuchi M et al (2007) Expression of retinaldehyde dehydrogenase 1 in the anterior pituitary glands of adult rats. *Cell Tissue Res* 329(2):321–327
- Guazzi S, Price M et al (1990) Thyroid nuclear factor 1 (TTF-1) contains a homeodomain and displays a novel DNA binding specificity. *EMBO J* 9(11):3631–3639
- Japon MA, Rubinstein M et al (1994) In situ hybridization analysis of anterior pituitary hormone gene expression during fetal mouse development. *J Histochem Cytochem* 42(8):1117–1125
- Kimura S, Hara Y et al (1996) The T/ebp null mouse: thyroid-specific enhancer-binding protein is essential for the organogenesis of the thyroid, lung, ventral forebrain, and pituitary. *Genes Dev* 10(1):60–69
- Kurotani R, Okumura S et al (2011) Secretoglobin 3A2 suppresses bleomycin-induced pulmonary fibrosis by transforming growth factor beta signaling down-regulation. *J Biol Chem* 286(22):19682–19692
- Kurotani R, Tomita T et al (2008) Role of secretoglobin 3A2 in lung development. *Am J Respir Crit Care Med* 178(4):389–398
- Lazzaro D, Price M et al (1991) The transcription factor TTF-1 is expressed at the onset of thyroid and lung morphogenesis and in restricted regions of the foetal brain. *Development* 113(4):1093–1104
- Leveque TF, Small M (1959) The relationship of the pituicyte to the posterior lobe hormones. *Endocrinology* 65:909–915
- Lew D, Brady H et al (1993) GHF-1-promoter-targeted immortalization of a somatotrophic progenitor cell results in dwarfism in transgenic mice. *Genes Dev* 7(4):683–693
- Liu W, Enwright JF 3rd et al (2002) CCAAT/enhancer binding protein alpha uses distinct domains to prolong pituitary cells in the growth 1 and DNA synthesis phases of the cell cycle. *BMC Cell Biol* 3:6
- Livak KJ, Schmittgen TD (2001) Analysis of Relative Gene Expression Data Using Real-Time Quantitative PCR and the $2^{-\Delta\Delta CT}$ Method. *Methods* 25(4):402–408
- Minoo P, Hamdan H et al (1995) TTF-1 regulates lung epithelial morphogenesis. *Dev Biol* 172(2):694–698
- Minoo P, Su G et al (1999) Defects in tracheoesophageal and lung morphogenesis in *Nkx2.1(-/-)* mouse embryos. *Dev Biol* 209(1): 60–71
- Mizuno K, Gonzalez FJ et al (1991) Thyroid-specific enhancer-binding protein (T/EBP): cDNA cloning, functional characterization, and structural identity with thyroid transcription factor TTF-1. *Mol Cell Biol* 11(10):4927–4933
- Nakamura K, Kimura S et al (2001) Immunohistochemical analyses of thyroid-specific enhancer-binding protein in the fetal and adult rat hypothalamic and pituitary glands. *Brain Res Dev Brain Res* 130(2): 159–166
- Niimi T, Keck-Waggoner CL et al (2001) UGRP1, a uteroglobin/Clara cell secretory protein-related protein, is a novel lung-enriched downstream target gene for the T/EBP/NKX2.1 homeodomain transcription factor. *Mol Endocrinol* 15(11): 2021–2036
- Ramji DP, Foka P (2002) CCAAT/enhancer-binding proteins: structure, function and regulation. *Biochem J* 365(Pt 3):561–575
- Schaufele F, Enwright JF 3rd et al (2001) CCAAT/enhancer binding protein alpha assembles essential cooperating factors in common subnuclear domains. *Mol Endocrinol* 15(10):1665–1676
- Sussel L, Marin O et al (1999) Loss of *Nkx2.1* homeobox gene function results in a ventral to dorsal molecular respecification within the basal telencephalon: evidence for a transformation of the pallidum into the striatum. *Development* 126(15):3359–3370
- Takuma N, Sheng HZ et al (1998) Formation of Rathke's pouch requires dual induction from the diencephalon. *Development* 125(23):4835–4840
- Tomita T, Kido T et al (2008) CAAT/enhancer-binding proteins alpha and delta interact with NKX2-1 to synergistically activate mouse secretoglobin 3A2 gene expression. *J Biol Chem* 283(37):25617–25627
- Yuan B, Li C et al (2000) Inhibition of distal lung morphogenesis in *Nkx2.1(-/-)* embryos. *Dev Dyn* 217(2):180–190



Relationships between oxygen consumption rate, viability, and subsequent development of *in vivo*-derived porcine embryos



N. Sakagami^{a,*}, K. Nishida^a, K. Akiyama^a, H. Abe^b, H. Hoshi^c, C. Suzuki^d, K. Yoshioka^d

^a Kanagawa Prefectural Livestock Industry Technology Center, Ebina, Kanagawa, Japan

^b Graduate School of Science and Engineering, Yamagata University, Yonezawa, Yamagata, Japan

^c Research Institute for the Functional Peptides, Higashine, Yamagata, Japan

^d Department of Production Diseases, National Institute of Animal Health, Tsukuba, Ibaraki, Japan

ARTICLE INFO

Article history:

Received 1 April 2014

Received in revised form 9 June 2014

Accepted 9 June 2014

Keywords:

Embryo

Non-surgical embryo transfer

Oxygen consumption rate

Pig

ABSTRACT

Oxygen consumption rate of *in vivo*-derived porcine embryos was measured, and its value as an objective method for the assessment of embryo quality was evaluated. Embryos were surgically collected 5 or 6 days after artificial insemination (AI), and oxygen consumption rate of embryos was measured using an embryo respirometer. The average oxygen consumption rate ($F \times 10^{14}/\text{mol s}^{-1}$) of the embryos that developed to the compacted morula stage on Day 5 (Day 0 = the day of artificial insemination) was 0.58 ± 0.03 (mean \pm standard error of the mean). The Day-6 embryos had consumption rates of 0.56 ± 0.13 , 0.87 ± 0.06 , and 1.13 ± 0.07 at the early blastocyst, blastocyst, and expanded blastocyst stages, respectively, showing a gradual increase as the embryos developed. Just after collection, the average oxygen consumption rates of embryos that hatched and of those that did not hatch after culture were 0.60 ± 0.04 and 0.50 ± 0.04 for Day 5 ($P = 0.08$) and 1.05 ± 0.09 and 0.77 ± 0.05 for Day 6 ($P < 0.05$), respectively. The value and probability of discrimination by measuring the oxygen consumption rates of embryos to predict their hatching ability after culture were 0.56 and 63.6% for Day-5 embryos and 0.91 and 68.4% for Day-6 blastocysts, respectively. When Day-5 embryos were classified based on the oxygen consumption rate and then transferred non-surgically to recipient sows, three of the seven sows, to which embryos having a high oxygen consumption rate (≥ 0.59) were transferred, became pregnant and farrowed a total of 20 piglets. However, none of the four sows, to which embryos having low oxygen consumption rate (< 0.59) were transferred, became pregnant. These results suggest that the viability of *in vivo*-derived porcine embryos and subsequent development can be estimated by measuring the oxygen consumption rate.

© 2015 Elsevier Inc. All rights reserved.

1. Introduction

An appropriate evaluation of embryo quality to select transferable embryos is important for the improvement of pregnancy rate after the embryo transfer. In general,

embryo selection is usually carried out by observation of their morphology, relying on the subjectivity of the technician. On the other hand, several objective methods for evaluating embryos have been reported, such as by identifying viable cells [1] and measuring metabolic activities such as glucose intake [2], carbon dioxide generation, [3] and oxygen consumption rate [4–7]. However, in these studies, measurement of single embryos appeared to be

* Corresponding author. Tel.: +81 46 238 4056; fax: +81 46 238 8634.
E-mail address: sakagami.semi@pref.kanagawa.jp (N. Sakagami).

difficult, and the treatments could potentially damage the embryos with harmful chemical exposures.

Because oxygen is consumed by oxidative phosphorylation and respiration in mitochondria and plays an important role in energy (ATP) production, respiration or oxygen consumption rate is considered as an appropriate index for the evaluation of embryo quality [8]. Recently, various methods have been reported for the measurement of mitochondrial oxygen consumption in embryos to evaluate their quality [8–14]. Moreover, high oxygen consumption rate of *in vivo*-derived bovine embryos was associated with a high conception rate after the embryo transfer [10,12,13]. However, there are only a few reports on the oxygen consumption measurement of porcine embryos [15–17] and/or on their subsequent developmental potential after the oxygen consumption measurements [15,16].

During the process of embryonic growth, mitochondria gain functional maturity, which is accompanied by a change in their morphology [18]. It has been reported that in bovine embryos, during the development from the morula to the blastocyst stage, mitochondria show a remarkable morphologic development highlighted by the expansion of cristae [18]. It is also clear that respiration activity changes corresponding to the development of mitochondria [18]. Although there are several reports about the differences in oxygen consumption rates between the developmental stages measured in single embryos [10–13,15–17], the optimum developmental stage for oxygen consumption measurement to assess embryo quality remained unclear. In cattle, the oxygen consumption rate remains low until the compacted morula stage and sharply increases thereafter until the expanded blastocyst stage [13,14]. Moreover, Shiku et al. [9] have reported that the hatching rate of *in vitro*-produced bovine morulae showing a high oxygen consumption rate ($>0.5 \times 10^{14}/\text{mol s}^{-1}$) was higher (68%) than that of morulae which consumed oxygen less than $0.5 \times 10^{14}/\text{mol s}^{-1}$ (0%). Therefore, it is suggested that measurement of oxygen consumption rate at the morula stage is a possible way to predict developmental ability of embryos. However, in porcine embryos, the relationship between oxygen consumption rate of embryos and their subsequent developmental ability *in vitro* and *in vivo* remained unknown.

Our present study was designed to measure the oxygen consumption rate of *in vivo*-derived porcine embryos using an embryo respirometer and clarify the relationships between the oxygen consumption rate and the developmental stage, the cell number, and viability of the embryos. Pregnancy outcomes after transfer to recipients of embryos classified with “high” or “low” levels of their oxygen consumption rates were also investigated.

2. Materials and methods

2.1. Embryo collection from gilts

All animal-related procedures followed in this study were done with the approval of the Institutional Animal Experiment Committee of Kanagawa Prefectural Agriculture Facilities. Embryos were collected from 25 prepubertal gilts (Large White, Landrace, or Yorkshire) following the procedures

described in our previous studies [15,19] with slight modifications. Superovulation was induced by an administration of eCG (Peamex 1500 IU intramuscular [im]; Sankyo, Tokyo, Japan) followed 72 hours later by an administration of hCG (Puberogen 500 IU im, Sankyo). The gilts were artificially inseminated twice, in the afternoon 1 day after hCG treatment and in the morning 2 days after hCG treatment. In the morning of Day 5 or 6 (Day 0 = the day of the first artificial insemination), the embryos were recovered from uterine horns by laparotomy under general anesthesia (4% to 5% [v:v] isoflurane) by flushing with a porcine oocyte/embryo collection medium [20] (POE-CM, Research Institute for the Functional Peptide [IFP], Yamagata, Japan). The embryos were kept in a porcine zygote medium (PZM-5, IFP) [21] under 5% CO₂, 5% O₂, and 90% N₂ at 38.5 °C until measurements.

2.2. Morphologic evaluation and measurement of embryo diameter

The collected embryos were classified by stages of development and quality standards of the Manual of the International Embryo Transfer Society [22], and only quality code 1 embryos were subjected to subsequent analyses. The diameters of embryos were measured using a digital camera for microscopes and attachment software (DXM1200 F and ACT-1; Nikon, Tokyo, Japan).

2.3. Measurement of the oxygen consumption rate

The oxygen consumption rate of the collected embryos was measured using an embryo respirometer (HV-405; IFP) according to the method of Abe et al. [14,18]. An embryo was placed at the bottom of the cone-shaped microwell on a respiration assay plate (RAP-1; IFP) filled with an embryo respiration assay medium (ERAM-2; IFP). A platinum microelectrode was set near the embryo, and a voltage of -0.6 V versus Ag/AgCl was applied to the microelectrode to reduce oxygen. The computer-controlled microelectrode scanned the z-axis (vertically) of the zona pellucida automatically at a moving speed of 30 $\mu\text{m/s}$ for a distance of 160 μm . Each embryo was measured twice by scanning two different lines, and the oxygen consumption rate was calculated using analytical software developed for estimating the oxygen consumption rate based on spherical diffusion [9]. Measurement of individual oxygen consumption rate was completed within 1 minute.

2.4. Evaluation of cell numbers in embryos

Some embryos were subjected to differential staining of inner cell mass (ICM) and trophectoderm (TE) by the method of Thouas et al. [23]. Briefly, embryos were stained by incubating in PBS containing 0.2% (v:v) Triton X-100 and 100 $\mu\text{g/mL}$ propidium iodide (P4170; Sigma Chemical, MO, USA) for 60 seconds and then stained and fixed by 25 $\mu\text{g/mL}$ of bisbenzimidazole (Hoechst 33342; Calbiochem, CA, USA) in ethanol, at 4 °C in the dark for at least 3 hours. The stained embryos were rinsed with antifade solution (SlowFade S2828; Invitrogen, Carlsbad, CA, USA), mounted on a slide glass, covered with a cover glass, and observed under an

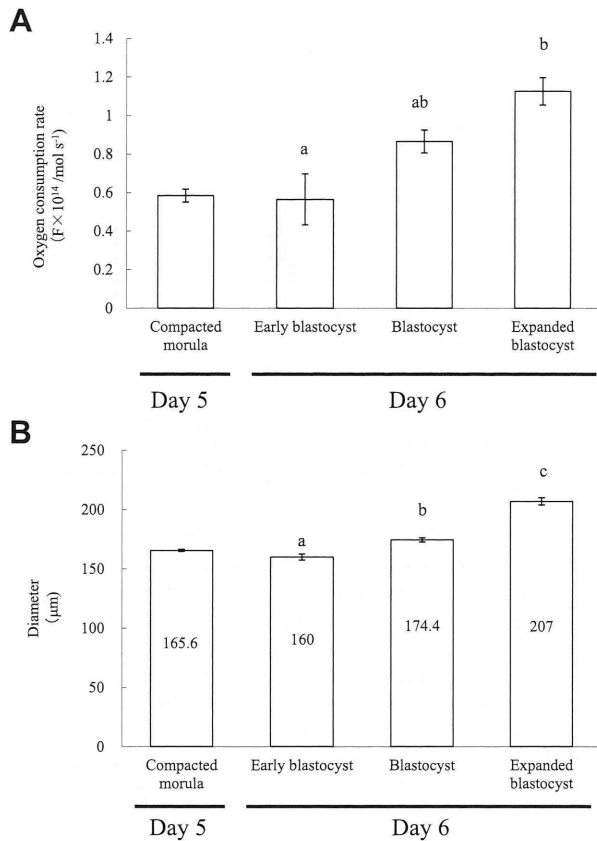


Fig. 1. Oxygen consumption rates (A) and diameter (B) of porcine embryos for each developmental stage. ^{a-c}Columns with different superscripts are significantly different ($P < 0.05$).

inverted fluorescent microscope through an ultraviolet filter to count the nuclei of the ICM and TE which were stained blue and pink, respectively.

2.5. Embryo transfer

Large White, Landrace, Yorkshire, and Berkshire sows (30.0 ± 3.0 [mean \pm standard error of the mean] months of age) were used for recipients of non-surgical embryo transfer, which was performed according to the method previously described by Yoshioka et al. [24]. The recipients were treated with eCG (Peamex 1000 IU im) in the morning of the next day of weaning and hCG (Puberogen 500 IU im)

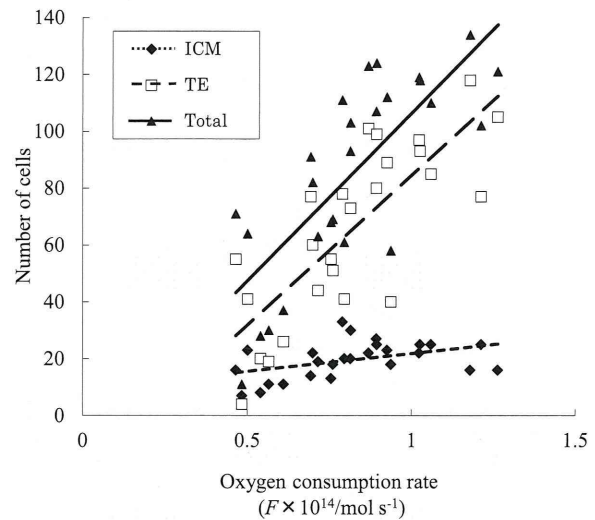


Fig. 2. Relationship between the oxygen consumption rate and the cell number in embryos collected on Day 6. Significant correlations were shown between the oxygen consumption rate and the number of inner cell mass (ICM) cells, trophoblast (TE) cells, and total number of cells (Number of ICM cells: $P < 0.05$, $r = 0.429$; TE cells: $P < 0.0001$, $r = 0.783$; and total number of cells: $P < 0.0001$, $r = 0.769$).

at 72 hours after eCG treatment. The embryos were transferred 5 days after hCG treatment. Porcine intrauterine transfer catheters (Takumi; Fujihira Industry Co., Tokyo, Japan) were used to transfer the embryos. The inner tube filled with porcine blastocyst medium (PBM; IFP) [25] was inserted through the outer sheath into the uterine horn as deep as possible. A 0.25-mL straw filled with PBM contained 13 to 21 embryos was attached to the outside end of the tube. The cotton plug part of the straw was removed using a straw cutter, and a syringe was attached to the cut end, from which 1 mL of PBM was squeezed to inject the content of the straw into the uterine horn. Pregnancy was diagnosed by ultrasonography at 35 days after embryo transfer. All pregnant recipients were allowed to carry their litters to term, and the farrowing rates and litter sizes were recorded.

2.6. Experimental design

2.6.1. Experiment 1: relationships between the oxygen consumption rate, the developmental stage, and the number of cells in *in vivo*-derived porcine embryos

The oxygen consumption rates of embryos at the compacted morula stage on Day 5 ($n = 29$) and at the early

Table 1

Correlation between the oxygen consumption rate and the cell number in Day-6 blastocysts ($n = 26$).

	Diameter of embryo	Oxygen consumption rate	Number of ICM cells	Number of TE cells	Total cell number	Respiratory activity per 100 cells
Diameter of embryo	1					
Oxygen consumption rate	0.809***	1				
Number of ICM cells	0.506**	0.429*	1			
Number of TE cells	0.918***	0.783***	0.577**	1		
Total cell number	0.902***	0.769***	0.697***	0.988***	1	
Respiratory activity per 100 cells	-0.532**	-0.371	-0.631**	-0.681***	-0.718***	1

* $P < 0.05$, ** $P < 0.01$, and *** $P < 0.0001$.

Abbreviations: ICM, inner cell mass; TE, trophoblast.

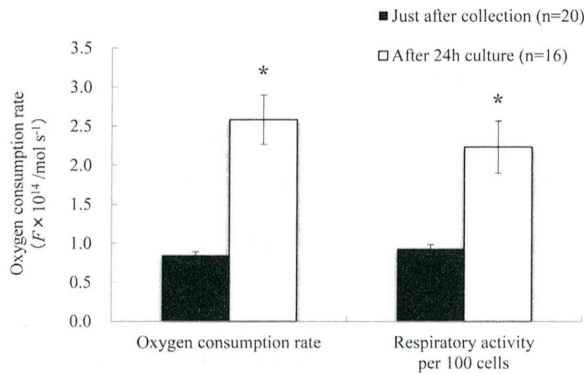


Fig. 3. Oxygen consumption rate and respiratory activity of embryos sampled on Day 6 just after collection and after 24 hours of culture. *Significantly different from Day-6 blastocysts ($P < 0.05$).

blastocyst ($n = 8$), blastocyst ($n = 27$), and the expanded blastocyst ($n = 39$) stages on Day 6 were measured and compared with the results of their morphologic evaluation. A total of 26 Day-6 embryos at the blastocyst stage were subjected to measure both of the oxygen consumption rate and cell numbers, from which the respiratory activity per 100 cells was calculated as the cellular respiratory activity of cells.

2.6.2. Experiment 2: oxygen consumption rate and cell numbers in in vivo-derived porcine embryos before and after in vitro culture

Day-6 embryos at the blastocyst stage ($n = 36$) were divided into two groups. Briefly, 20 blastocysts were evaluated for oxygen consumption rate, and then their cell numbers were counted immediately. The rest of the blastocysts ($n = 16$) were measured for oxygen consumption rate and then cultured in a PBM in a Reproplate (IFP) individually, for 24 hours under 5% CO_2 , 5% O_2 , and 90% N_2 at 38.5 °C. The number of cells in these blastocysts was also measured after culture.

2.6.3. Experiment 3: oxygen consumption rate of the in vivo-derived porcine embryos and their subsequent developmental potential

The Day-5 compacted morulae ($n = 33$) and the Day-6 blastocysts ($n = 38$) after measurement of the oxygen consumption rate were cultured in PBM in a Reproplate individually for 48 hours (Day-5 compacted morulae) or 24 hours (Day-6 blastocysts). After culture, the hatching from the zona pellucida was investigated.

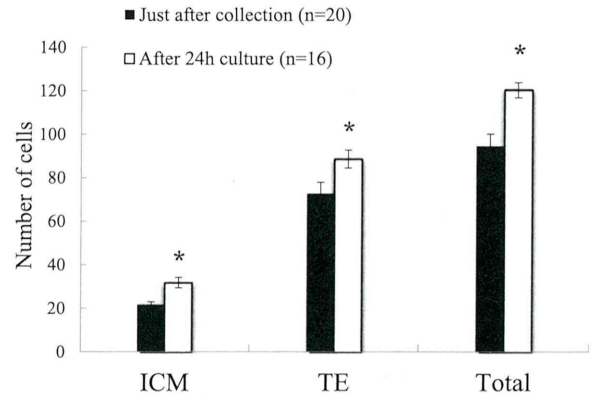


Fig. 4. Comparison of the cell number in embryos sampled on Day 6 just after collection and after 24 hours of culture. *Significantly different from freshly collected Day-6 blastocysts ($P < 0.05$). ICM, inner cell mass; TE, trophoctoderm.

2.6.4. Experiment 4: oxygen consumption of the in vivo-derived porcine embryo and conception rate

The compacted morulae and early blastocysts collected on Day 5 were measured for oxygen consumption rate and then transferred to recipients non-surgically to investigate the conception performance. Embryos were divided into two groups according to their oxygen consumption rates: average oxygen consumption of less than $0.58 \times 10^{14} / \text{mol s}^{-1}$ (the lower oxygen consumption group) and more than $0.59 \times 10^{14} / \text{mol s}^{-1}$ (the higher oxygen consumption group).

2.7. Statistical analysis

Data were statistically processed using a computer program for statistical processing SPSS (SPSS 16.0J. User's Guide; SPSS, Tokyo, Japan). ANOVA was performed followed by the Tukey HSD test. Linear relationships and correlation coefficients between the oxygen consumption rate and the cell numbers of embryos were determined by simple regression analysis and Pearson product-moment correlation coefficient analysis, respectively. The Fisher exact probability test was used to compare the conception rates, and a P value of less than 0.05 was considered statistically significant.

Embryos that hatched and those which did not hatch from the zona pellucida after culture were compared for their mean oxygen consumption rates at the time of collection as the explanatory variable, determining the difference from the mean for each embryo and calculating the discriminant function using the linear discriminant

Table 2

Correlation between the oxygen consumption rate and the cell number in Day-6 blastocysts after 24 hours of culture ($n = 16$).

	Oxygen consumption rate	Number of ICM cells	Number of TE cells	Total cell number	Respiratory activity per 100 cells
Oxygen consumption rate	1				
Number of ICM cells	0.232	1			
Number of TE cells	-0.506*	-0.536*	1		
Total cell number	-0.440	0.050	0.817***	1	
Respiratory activity per 100 cells	0.974***	0.220	-0.638**	-0.605*	1

* $P < 0.05$, ** $P < 0.01$, and *** $P < 0.001$.

Abbreviations: ICM, inner cell mass; TE, trophoctoderm.

Table 3Oxygen consumption rates of Day-5 and -6 porcine embryos at collection and hatching from the zona pellucida after culture.^c

Embryo collection	Hatching from the zona pellucida after culture	Number of embryos examined	Oxygen consumption rate ($F = 10^{14}/\text{mol s}^{-1}$)
Day 5	Not hatched	17	0.50 ± 0.04
	Hatched	16	0.60 ± 0.04
	Total	33	0.55 ± 0.03
Day 6	Not hatched	16	0.77 ± 0.05^a
	Hatched	22	1.05 ± 0.09^b
	Total	38	0.93 ± 0.06

^{a,b}Values in the same column with different superscripts are significantly different ($P < 0.05$).^c Day-5 and -6 embryos were checked for hatching after 48 and 24 hours, respectively, of culture in porcine blastocyst medium.

function. The probability of discrimination was then calculated from the determined discriminant function using the cross table of the discrimination probability.

3. Results

3.1. Experiment 1

The average oxygen consumption rate ($F \times 10^{14}/\text{mol s}^{-1}$) of the Day-5 embryos was 0.58 ± 0.03 for the compacted morula stage. Oxygen consumption rates of Day-6 embryos were 0.56 ± 0.13 , 0.87 ± 0.6 , and 1.13 ± 0.07 for the early blastocyst, blastocyst, and expanded blastocyst stages, respectively, and the value at the expanded blastocyst stage was significantly higher than that at the early blastocyst stage (Fig. 1A). On Day 6, the diameter of the embryos significantly increased with the progress of developmental stages (Fig. 1B).

Significant correlations were detected between the oxygen consumption rate of individual embryos and their diameter and cell numbers (in terms of ICM, TE, and total cells as well; Table 1). The oxygen consumption rate showed highly positive correlations with the total and TE cell numbers (Table 1 and Fig. 2).

3.2. Experiment 2

The oxygen consumption (2.58 ± 0.32) and respiration activity per 100 cells (2.23 ± 0.33) of embryos cultured for 24 hours from Day 6 were significantly higher than those of Day-6 blastocysts (0.85 ± 0.04 and 0.93 ± 0.05 , respectively; Fig. 3). The total number of cells and the number of ICM and TE cells of Day-6 embryos after culture were also significantly greater than those of embryos before the culture (Fig. 4). The oxygen consumption rate of embryos (cultured from Day 6 for 24 hours) did not show significant correlation with the total cell numbers and the numbers of

ICM cells of the embryos after 24 hours culture, but there was a significant correlation between the oxygen consumption rate and the respiratory activity after the culture (Table 2).

3.3. Experiment 3

The oxygen consumption rates of the porcine embryos collected on Day 5 or 6 and the culture outcome are shown in Table 3. In Day-5 embryos, the oxygen consumption rate before culture was tendentially higher in those embryos that hatched after 48 hours of culture compared with those that did not hatch ($P = 0.08$). In Day-6 blastocysts, the oxygen consumption rates of those that hatched after 24 hours culture were higher than those of that did not hatch ($P < 0.05$). The discrimination probabilities of the Day-5 and -6 embryos, which were calculated using the values as the standards and the cross table of the discrimination probability, were 63.6% and 68.4%, respectively (Table 4).

3.4. Experiment 4

The embryos were transferred into each of 11 sows, of which three became pregnant (Table 5). Pregnancy was not obtained in any of the recipients in which embryos with low oxygen consumption rates were transferred. However, three of the seven recipients into which embryos with high oxygen consumption rates were transferred became pregnant. The three pregnant sows delivered 6.3 piglets on average (6, 3, and 11), and the mean gestation period was 116.3 ± 0.9 days.

4. Discussion

The present study clearly demonstrates that porcine embryos that could hatch after the subsequent culture

Table 4

Number of the Day-5 and -6 embryos resulted in false or true of whether hatched from the zona pellucida for each oxygen consumption class and the discrimination probabilities.

Embryo collection (number of embryos)	Prediction (number of embryos)	Number of embryos (%)		Discrimination probability (%)
		False	True	
Day 5 (33)	Not hatching (19)	7 (43.8)	12 (70.6)	63.6
	Hatched (14)	5 (29.4)	9 (56.3)	
Day 6 (38)	Not hatching (20)	8 (36.4)	12 (75.0)	68.4
	Hatched (18)	4 (25.0)	14 (63.6)	

Table 5
Conception rate of the embryos of each oxygen consumption class.

	Number of sows (number of embryos transferred)	Mean oxygen consumption rate ($F \times 10^{14}/\text{mol s}^{-1}$) ^c	Number of pregnant sows (%)	Number of farrowed sows (%)	Number of piglets delivered ($\delta:\text{♀}$)	Percentage of piglets born/embryo transferred (%)
High oxygen consumption	7 (118)	0.89 ± 0.03^a	3 (42.9)	3 (42.9)	20 ^d (12:8 ^d)	16.9
Low oxygen consumption	4 (58)	0.52 ± 0.02^b	0 (0)	0 (0)	0	0
Total	11 (176)	0.77 ± 0.03	3 (27.3)	3 (27.3)	20 ^d (12:8 ^d)	11.4

^{a,b}Values in the same column with different superscripts are significantly different ($P < 0.05$).

^c Mean \pm standard error of the mean.

^d Two piglets were stillborn.

showed higher oxygen consumption rates at the time of collection than those embryos that did not hatch. Oxygen consumption rate of the embryos at the blastocyst stage correlated with the number of cells. Moreover, piglets could be obtained by non-surgical transfer of embryos with high oxygen consumption rates.

These results corroborate with previous reports in bovine embryos, describing the correlation between their oxygen consumption rate and their viability [9–14] and conception rate [10,12,13]. Shiku et al. [9] examined the oxygen consumption of morula-stage bovine embryos and their subsequent hatching from the zona pellucida and reported that the hatching rate was higher in embryos showing oxygen consumption rates of at least 0.5 compared with those showing consumption rates lower than 0.5.

Our results revealing that Day-5 or -6 porcine embryos with high oxygen consumption rates are likely to show a high viability thereafter *in vitro* suggest that also in pigs, the oxygen consumption rate in freshly collected embryos may be a potent predictor for embryo viability.

The determining oxygen consumption values were calculated using the linear discriminant function and the oxygen consumption before the culture as the explanatory variable. The discrimination value for the hatched or not hatched in Day-5 and Day-6 embryos was 0.56 and 0.91, showing a discrimination probability of 63.6% and 68.4%, respectively. It suggests that both on Days 5 (at the compacted morula stage) and 6 (at the blastocyst stage), embryos could be discriminated for hatching ability by the measurement of their oxygen consumption rate. However, the oxygen consumption rate of Day-6 embryos at the expanded blastocyst stage was significantly higher than those at the early blastocyst stage, indicating that the oxygen consumption rate of porcine embryos on Day 6 increased greatly with the progress of development. In fact, there is a large variation in the developmental stage of embryos collected on Day 6, which should be considered when comparing oxygen consumption rates to assess embryo quality. Thus, the discrimination for the hatching ability by the measurement of oxygen consumption rate is may be appropriate 5 days after artificial insemination for the selection of transferable porcine embryos with high quality.

When we transferred Day-5 embryos (compacted morulae and early blastocysts) after the measurement of the oxygen consumption rate, 42.9% (3 of 7) of the recipients, to which embryos with high oxygen consumption rates were

transferred, became pregnant and farrowed healthy piglets. In contrast, no pregnancy was obtained in the group to which the embryos with low oxygen consumption rates were transferred (0/4). Thus, embryos with high oxygen consumption rate may have superior conception ability compared with those with low oxygen consumption rate. Our overall result of pregnancy after non-surgical embryo transfer (27.3%) is similar to that of previous report (25% farrowing rate) on the transfer of *in vitro*-produced porcine embryos using the same deep intrauterine catheter instrument [25].

The oxygen consumption rate of blastocyst stage embryos on Day 6 showed a positive correlation with both the total cell numbers and the numbers of TE cells. Particularly, the embryos of higher oxygen consumption rate were found to have larger numbers of TE cells, suggesting the possibility of estimating the cell number from the oxygen consumption rate. In accordance with our results, Sugimura et al. [16] mentioned that anomalous low oxygen consumption rate in porcine SCNT blastocysts could be a sign of limited hatchability, which may be responsible for the low TE cell number and high apoptosis incidence. They also suggested that low oxygen consumption of Day-5 porcine SCNT blastocysts in the number of low TE cell may involve the high incidence of apoptosis in Day-7 blastocysts [16]. Furthermore, it has been reported that nitric oxide, which induces oxidative stress and apoptosis, and diamide-induced apoptosis may limit oxygen consumption at the blastocyst stage in the mouse embryo [26,27]. These findings suggest that the viability of TE cells may predominantly determine the oxygen consumption rate and greatly affect the porcine embryo quality.

The actual size of the embryo may also affect its oxygen consumption rate. It has been reported that *in vitro*-produced bovine blastocysts of larger diameter have higher oxygen consumption rate compared with smaller embryos [12]. Also, the positive correlation between the cell numbers in Day-7 bovine blastocyst and the length of their derivative conceptuses after transfer on Day 14 have been reported [28]. In pigs, asynchrony of TE elongation from Day 11 to 12 of pregnancy is evident in porcine concepti, and rapid progression through this phase has been associated with conceptus competency [29]. In the present study, the significant correlation was also observed between the oxygen consumption rate and the diameter of porcine embryo, suggesting that the diameter of the embryos was related to the quality of embryos.

Although, there was no significant correlation between the oxygen consumption rate and the respiratory activity in freshly collected Day-6 blastocysts, there was a significant correlation between the oxygen consumption rate and the respiratory activity of embryos after culture for 24 hours. These findings suggest that the oxygen consumption in freshly collected Day-6 embryos was more closely related to the actual number of cells rather than cellular respiratory activity which was correlated to oxygen consumption after additional culture.

In conclusion, the oxygen consumption rate of the *in vivo*-derived porcine embryos was significantly increased with the progress of development from the morula to the expanded blastocyst stage, and the embryos that hatched after additional culture showed higher rates of oxygen consumption than those that did not hatch. A significant correlation was observed in the Day-6 embryos between the oxygen consumption rate and the number of cells. After embryo transfer, successful pregnancies were only achieved with embryos showing high oxygen consumption rate, which, in turn, could develop to normal piglets. Therefore, the oxygen consumption by an embryo is likely to be related to its subsequent survival and conception, suggesting the possibility for the objective evaluation of the developmental capacity of an embryo based on its oxygen consumption rate.

Acknowledgments

The authors would like to thank Y. Shimizu, T. Kashiwagi, and K. Tani for technical assistance. This work was supported in part by the Program for Promotion of Basic and Applied Researches for Innovations in Bio-oriented Industry from Bio-oriented Technology Research Advancement Institution (BRAIN) and Grant-in-Aid for Scientific Research (25292184) from the Japan Society for the Promotion of Science (JSPS).

References

- [1] Schilling E, Dopke HH. A rapid diagnostic test for the viability of early cattle and rabbit embryos using diacetyl-fluorescein. *Naturwissenschaften* 1978;65:658–9.
- [2] Renard JP, Philippon A, Menezo Y. In-vitro uptake of glucose by bovine blastocysts. *J Reprod Fertil* 1980;58:161–4.
- [3] Brinster RL. Carbon dioxide production from glucose by the preimplantation mouse embryo. *Exp Cell Res* 1967;47:271–7.
- [4] Mills RM, Brinster RL. Oxygen consumption of preimplantation mouse embryos. *Exp Cell Res* 1967;47:337–44.
- [5] Magnusson C, Hillensjo T, Hamberger L, Nilsson L. Oxygen consumption by human oocytes and blastocysts grown in vitro. *Hum Reprod* 1986;1:183–4.
- [6] Overstorm EW, Doby RT, Dobrinsky J, Roche JF, Boland MP. Viability and oxidative metabolism of the bovine blastocyst. *Theriogenology* 1992;37:269.
- [7] Houghton FD, Thompson JG, Kennedy CJ, Leese HJ. Oxygen consumption and energy metabolism of the early mouse embryo. *Mol Reprod Dev* 1996;44:476–85.
- [8] Lopes AS, Wrenzycki C, Ramsing NB, Herrmann D, Niemann H, Løvendahl P, et al. Respiration rates correlate with mRNA expression of G6PD and GLUT1 genes in individual bovine in vitro-produced blastocysts. *Theriogenology* 2007;68:223–36.
- [9] Shiku H, Shiraishi T, Ohya H, Matsue T, Abe H, Hoshi H, et al. Oxygen consumption of single bovine embryos probed by scanning electrochemical microscopy. *Anal Chem* 2001;73:3751–8.
- [10] Sakagami N, Akiyama K, Nakazawa Y. The relationship between oxygen consumption rate and pregnancy rate of bovine embryos. *Reprod Fertil Dev* 2007;19:225 (abstract).
- [11] Lopes AS, Larsen LH, Ramsing N, Løvendahl P, Råty M, Peippo J. Respiration rates of individual bovine in vitro-produced embryos measured with a novel, non-invasive and highly sensitive micro-sensor system. *Reproduction* 2005;30:669–79.
- [12] Lopes AS, Madsen SE, Ramsing N, Løvendahl P, Greve T, Callesen H. Investigation of respiration of individual bovine embryos produced in vivo and in vitro and correlation with viability following transfer. *Hum Reprod* 2007;22:558–66.
- [13] Lopes AS, Greve T, Callesen H. Quantification of embryo quality by respirometry. *Theriogenology* 2007;67:21–31.
- [14] Abe H, Shiku H, Aoyagi S, Hoshi H. In vitro culture and evaluation of embryos for production of high quality bovine embryos. *J Mamm Ova Res* 2004;21:22–30.
- [15] Sakagami N, Yamamoto T, Akiyama K, Nakazawa Y, Kojima N, Nishida K, et al. Viability of porcine embryos after vitrification using water-soluble pullulan films. *J Reprod Dev* 2010;56:279–84.
- [16] Sugimura S, Yokoo M, Yamanaka K, Kawahara M, Moriyasu S, Wakai T, et al. Anomalous oxygen consumption in porcine somatic cell nuclear transfer embryos. *Cell Reprogram* 2010;12:463–74.
- [17] Sturmey RG, Leese HJ. Energy metabolism in pig oocytes and early embryos. *Reproduction* 2003;126:197–204.
- [18] Abe H, Matsuzaki S, Hoshi H. Ultrastructural differences in bovine morulae classified as high and low qualities by morphological evaluation. *Theriogenology* 2002;57:1273–83.
- [19] Nakazawa Y, Misawa H, Fujino Y, Tajima S, Misumi K, Ueda J, et al. Effect of volume of non-surgical embryo transfer medium on ability of porcine embryos to survive to term. *J Reprod Dev* 2008;54:30–4.
- [20] Yoshioka K, Suzuki C, Onishi A. Defined system for in vitro production of porcine embryos using a single basic medium. *J Reprod Dev* 2008;54:208–13.
- [21] Yoshioka K, Suzuki C, Tanaka A, Anas IM, Iwamura S. Birth of piglets derived from porcine zygotes cultured in a chemically defined medium. *Biol Reprod* 2002;66:112–9.
- [22] IETS. Stringfellow DA, Seide SM, editors. Manual of the International Embryo Transfer Society. Third Edition. USA: International Embryo Transfer Society; 1998. p. 167–70.
- [23] Thouas GA, Korfiatis NA, French AJ, Jones GM, Trounson AO. Simplified technique for differential staining of inner cell mass and trophoctoderm cells of mouse and bovine blastocysts. *Reprod BioMedicine Online* 2001;3:25–9.
- [24] Yoshioka K, Noguchi M, Suzuki C. Production of piglets from *in vitro*-produced embryos following non-surgical transfer. *Anim Reprod Sci* 2012;131:23–9.
- [25] Mito T, Yoshioka K, Yamashita S, Suzuki C, Noguchi M, Hoshi H. Glucose and glycine synergistically enhance the in vitro development of porcine blastocysts in a chemically defined medium. *Reprod Fertil Dev* 2011;24:443–50.
- [26] Manser RC, Leese HJ, Houghton FD. Effect of inhibiting nitric oxide production on mouse preimplantation embryo development and metabolism. *Biol Reprod* 2004;71:528–33.
- [27] Trimarchi JR, Liu L, Porterfield DM, Smith PJ, Keefe DL. Oxidative phosphorylation-dependent and -independent oxygen consumption by individual preimplantation mouse embryos. *Biol Reprod* 2000;62:1866–74.
- [28] O'Hara L, Forde N, Kelly AK, Lonergan P. Effect of bovine blastocyst size at embryo transfer on Day 7 on conceptus length on Day 14: can supplementary progesterone rescue small embryos? *Theriogenology* 2014;81:1123–8.
- [29] Blomberg LA, Schreier L, Li RW. Characteristics of peri-implantation porcine concepti population and maternal milieu influence the transcriptome profile. *Mol Reprod Dev* 2010;77:978–89.